表4　血清中フェンタニル濃度の薬物動態パラメータ

		$AUC_{216-240}$ (pg·hr/mL)	$AUC_{168-240}$ (pg·hr/mL)	剥離後の $t_{1/2}$ (hr)
2 mg 群 (n=7)	平均値	19961	56761	31.31
	標準偏差	9222	22615	9.78
4 mg 群 (n=5)	平均値	34102	101253	25.73
	標準偏差	14409	34943	7.00

表5　1日1回，10日間反復貼付試験成績より算出した累積係数

	2 mg 群 (n=7)			4 mg 群 (n=5)		
	C_{24} (pg/mL)	C_{240} (pg/mL)	累積係数	C_{24} (pg/mL)	C_{240} (pg/mL)	累積係数
平均値	277	864	3.2	579	1506	2.7
標準偏差	87	448	1.2	278	681	1.1

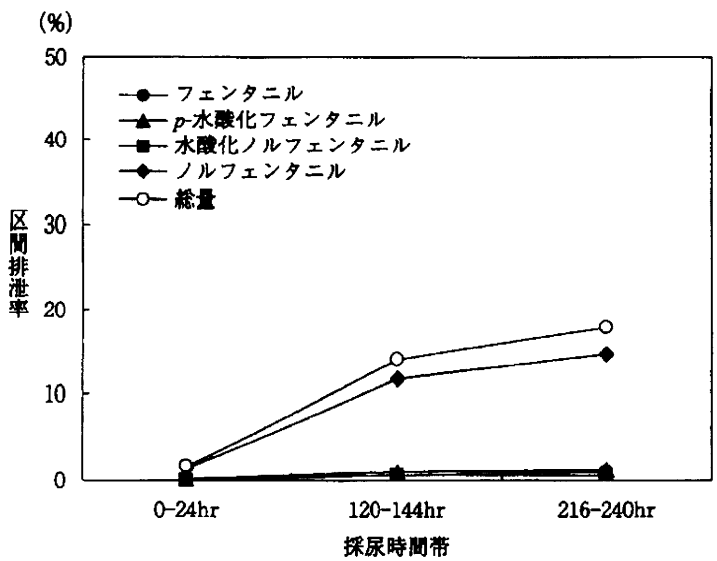

図5　2 mg群のフェンタニルおよび代謝物の平均区間排泄率（n=7，β-グルクロニダーゼ処理後）

くなっていたことから，*p*-水酸化フェンタニルは抱合体として尿中に排泄されるものと考えられた。フェンタニルおよびこれら代謝物の尿中排泄量は用量に比例して増加し，また，尿中代謝物の組成は用量にかかわらずほぼ一定であったことから，反復貼付においても代謝パターンは用量により変化せず一定であると考えられた。

4．モルヒネからの切り替え試験（第Ⅱ相）

薬物動態解析対象集団は117例であった。性別の内訳は男性が69例，女性が48例，年齢の平均値±標準偏差は63.4±12.1歳，身長は159.8±8.9cm，体重は51.5±10.3kgであった。

HFT-290 1～8 mgを1日1回，9日間反復貼付したとき，血清中フェンタニル濃度はいずれの用量においても貼付後3日（72時間）以降でほぼ一定

であった（図6）。

また，治験期間中にHFT-290を3日間以上同一用量（1～10mg）で貼付した患者を対象として，同一用量貼付時の最終回貼付時における剥離直前の血清中フェンタニル濃度を用いて，血清中フェンタニル濃度の用量比例性の検討をPowerモデルにより行った（$y=a\cdot x^{\beta}$を用いて，対数変換後の回帰式：$\log(y)=\alpha+\beta\cdot\log(x)$により回帰係数$\alpha$および$\beta$を推定した）。

その結果，回帰係数βは1.03であり，また，その95%信頼区間は0.89～1.17と1を含んでいたことから，HFT-290反復貼付後の定常状態における血清中フェンタニル濃度は用量（1～10mg）に比例して増加することが示唆された（図7）。

5．薬物動態および薬力学検討試験（第Ⅱ相）

薬物動態解析対象集団は25例（H1群が10例，H3群が8例およびD3群が7例）であった。性別の内訳は男性が14例（H1群が6例，H3群が4例およびD3群が4例），女性が11例（H1群が4例，H3群が4例およびD3群が3例），年齢の平均値±標準偏差はH1群が54.6±6.8歳，H3群が55.5±8.2歳およびD3群が56.9±6.4歳であった。身長はH1群が162.6±5.6cm，H3群が162.8±10.5cm，D3群が161.1±10.3cm，体重はH1群が55.9±11.6kg，H3群が52.4±11.7kg，D3群が49.7±9.6kgであった。

H1群，H3群およびD3群の血清中フェンタニル濃度の推移パターンは3群間で異なり，H1群では貼付後96時間以降の各評価時期においてほぼ一定の血清中フェンタニル濃度を維持していたのに対し，H3群では貼り替え後24時間から72時間にかけて徐々に低下する傾向を示した。D3群の血清中フェンタニル濃度はH1群に近似していた。また，D3群の血清中フェンタニル濃度もH3群と同様に貼り替え後24時間から72時間にかけてやや低下する傾向を示した（図8）。

$AUC_{144-216}$はH1群が48681.6pg·hr/mL，H3群が26524.5pg·hr/mL，D3群が39226.0pg·hr/mLであった（表6）。

剥離後の製剤中の残存率より算出した吸収率はH1群が63.1±19.4%，H3群が77.5±10.6%およびD3群が62.3±10.3%であった。

6．単回貼付成績からの予測値と反復貼付試験の実測値の比較

単回貼付時と反復貼付時の薬物動態の比較を，単

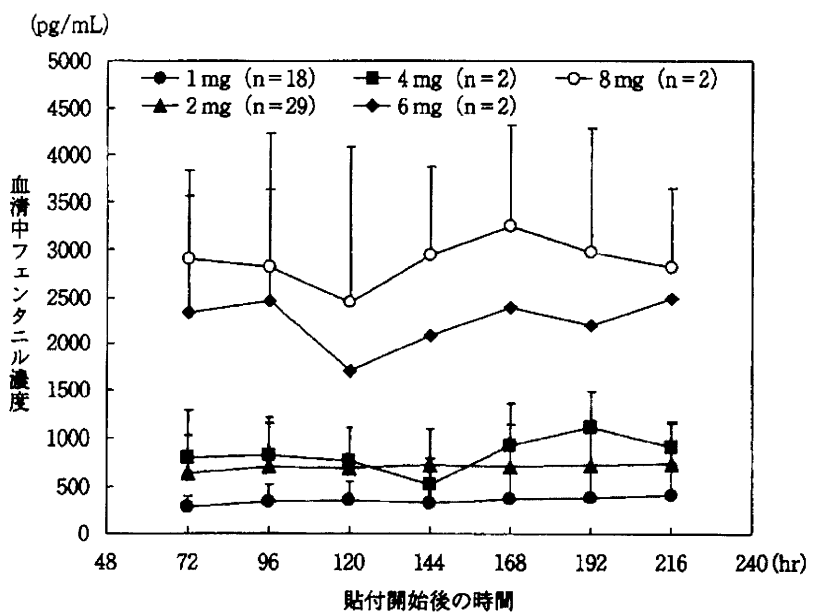

図6　血清中フェンタニル濃度推移（平均値＋標準偏差，1 mg群の72および216時間後はn=17，2 mg群の144時間以降はn=28，6 mg群の120時間以降はn=1）

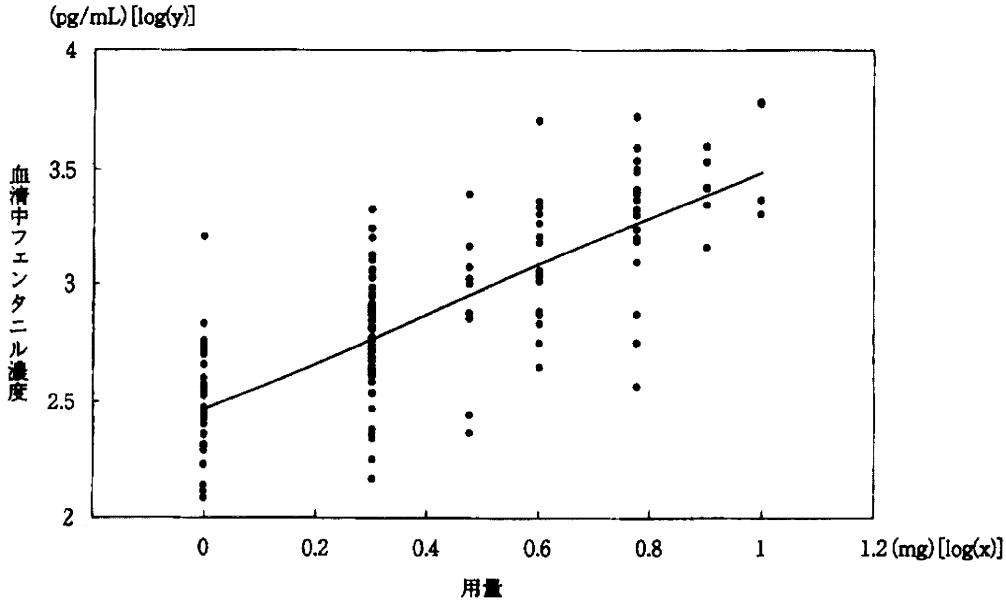

図7　用量比例性の検討

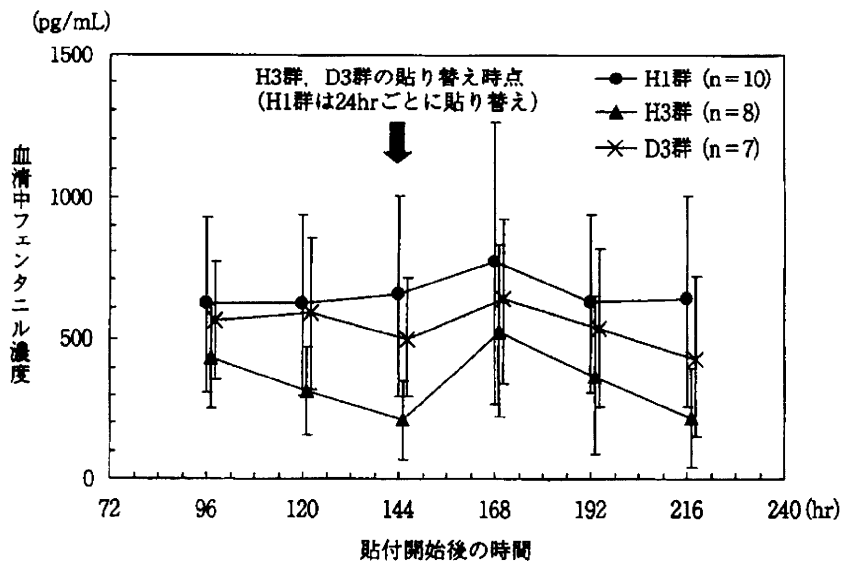

図8　群別の血清中フェンタニル濃度推移（平均値±標準偏差，D3群は144時間以降，n=6）

回貼付成績から予測される血清中フェンタニル濃度（重ね合わせ法によるシミュレーション値）と反復貼付時の実測値との比較により行ったところ，単回貼付成績からの予測値と反復貼付時の実測値は近似しており，単回貼付時の薬物動態から予測可能な範囲であったと考えられた（図9，10）。

Ⅲ　結論および考察

HFT-290は，フェンタニルクエン酸塩を有効成分とし，臨床使用時の利便性に優れる1日1回貼付の経皮吸収型製剤として久光製薬株式会社が創製し

表6　群別の $AUC_{144-216}$

		$AUC_{144-216}$ (pg・hr/mL)
H1群　(n=10)	平均値	48681.6
	標準偏差	26881.7
H3群　(n=8)	平均値	26524.5
	標準偏差	17350
D3群*　(n=6)	平均値	39226
	標準偏差	17693.2

*：1例は有害事象により中止したため，パラメータの算出から除外

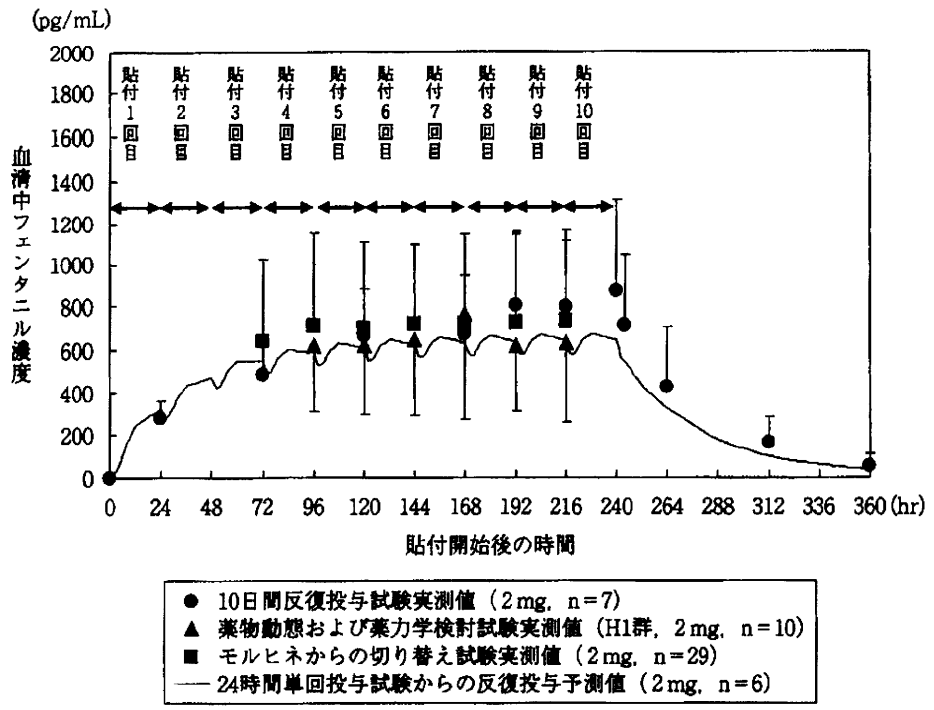

図9　24時間単回貼付試験からの血清中フェンタニル濃度予測値と1日1回，10日間反復貼付時の血清中フェンタニル濃度実測値の比較（実測値については平均値＋標準偏差または平均値－標準偏差，モルヒネからの切り替え試験は144時間以降，n=28）

たマトリクスタイプの製剤である。HFT-290の1日1回貼付時の薬物動態特性の確認に加え，本剤の用法の妥当性を確認することを目的として，1日1回貼付と3日に1回貼付の2用法について単回および反復貼付試験を実施した。

HFT-290 2および4 mgを24時間単回貼付したとき，血清中フェンタニル濃度は緩やかに上昇し，24時間で最高濃度に達した後，製剤剥離後は半減期30時間前後で消失した。この結果から，HFT-290貼付後の血清中フェンタニル濃度は急激な上昇をきたすことなく緩やかに上昇するため，安全性の面で好ましいと考えられた。また，C_{max}および$AUC_{0-\infty}$は用量に比例して増加し，t_{max}および剥離後の$t_{1/2}$はいずれの用量でも大きな差は認められなかった。

剥離後の製剤中に残存するフェンタニルクエン酸塩量から算出した吸収率は約60～70%であり，そ

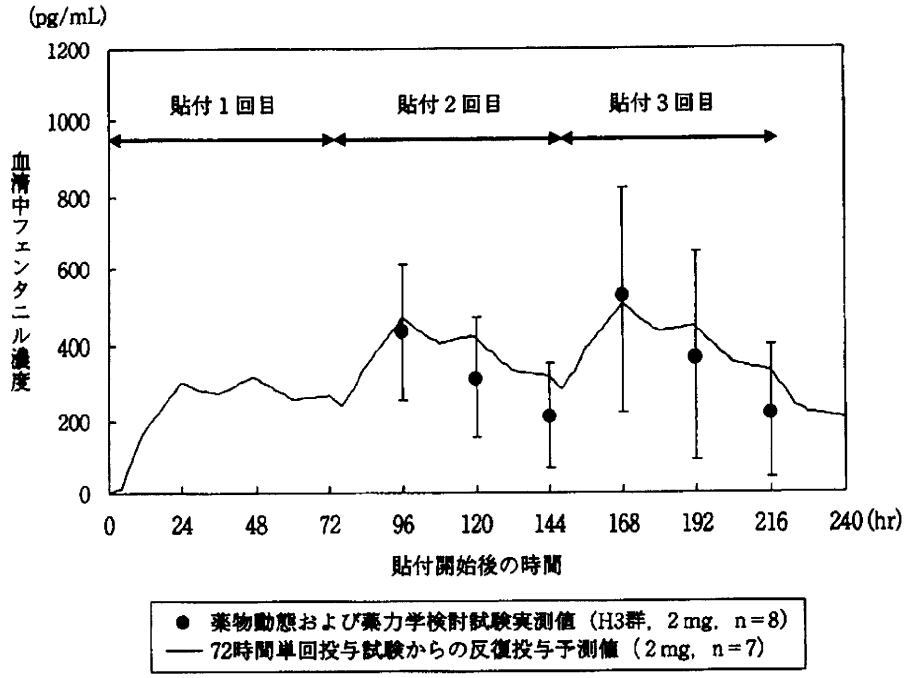

図10　72時間単回貼付試験からの血清中フェンタニル濃度予測値と3日に1回，9日間反復貼付時の血清中フェンタニル濃度実測値の比較（実測値については平均値±標準偏差）

の変動係数（%CV）も20%前後であったことから，安定した薬物放出能を有する製剤であると考えられた。また，剥離後の製剤中に残存するフェンタニルクエン酸塩量から算出した吸収量の変動係数は，単回貼付時における$AUC_{0-\infty}$の変動係数（40～50%）に比べ小さい傾向を示していた。フェンタニルは主に肝臓のCYP3A4により代謝されるが[10)11)]，ヒト肝臓におけるCYP3A4含量の変動係数は53%[12)]，外科手術患者への静注時の全身クリアランスの変動係数は約43%であり[13)]，HFT-290貼付後の薬物動態パラメータの変動係数と大きく異ならないことから，HFT-290貼付後の薬物動態の個体間変動は主に個体ごとの肝代謝能に依存するものと考えられた。

HFT-290を1日1回反復貼付した際の血清中フェンタニル濃度は，貼付後3日（約72時間）～5日（約120時間）でほぼ一定となった。また，貼付後3日以降の定常状態における血清中フェンタニル濃度は1～10mgの用量の範囲で比例して増加しており，この用量の範囲において線形の薬物動態が確認された。

HFT-290を反復貼付したときの製剤剥離後の$t_{1/2}$の平均は30時間前後（最小値17時間～最大値45時間）であり，単回貼付時の剥離後半減期と大きな違いは認められなかった。また，反復貼付時の剥離後の製剤中の残存率より算出した吸収率は単回貼付時の吸収率と同程度であった。さらに，単回貼付成績から予測される血清中フェンタニル濃度（重ね合わせ法によるシミュレーション値）と反復貼付時の実測値は近似しており，反復貼付時の血清中フェンタニル濃度は単回貼付時の薬物動態から予測可能な範囲であったと考えられた。すなわち，HFT-290の1日1回の反復貼付において，血清中フェンタニル濃度に蓄積性は認められないことが確認された。

また，HFT-290反復貼付後のフェンタニルおよび各代謝物の尿中排泄に関して，尿中主代謝物はノルフェンタニルであり，*p*-水酸化フェンタニルは抱合体として尿中に排泄されるものと考えられた。フェンタニルおよびこれら代謝物の尿中排泄量は用量に比例して増加し，また，尿中代謝物の組成は用量，貼付回数にかかわらずほぼ一定であったことから，反復貼付においても代謝に大きな変動はなく，

一定であると考えられた。

一方，HFT-290（2，4および8 mg）を72時間単回貼付したとき，血清中フェンタニル濃度は24～30時間（中央値）で最高に達し，以降，貼付中にもかかわらず低下が認められた。製剤剥離後の半減期は27～38時間であり，24時間貼付時と同程度の消失半減期を示した。C_{max}および$AUC_{0-\infty}$ともに用量に比例して増加し，またt_{max}および製剤剥離後の$t_{1/2}$はいずれの用量でも大きな差は認められなかった。HFT-290を72時間貼付したとき，貼付中の血清中フェンタニル濃度に関して日内変動が観察された。同様の血中濃度の日内変動は既承認のフェンタニル経皮吸収型製剤やロキソプロフェン経皮吸収型製剤においても報告されている[5)14)]。皮膚温や皮膚pHなどは日内変動することが報告されており[15)]，薬物動態的な日内変動に肝血流量や肝代謝酵素活性などに関する日内変動が関与している可能性も示唆されている[16)]。フェンタニルを経皮投与したとき，体温や外部熱源の上昇で吸収が増加することが報告されており[17)]，また，フェンタニルは主に肝臓で代謝されることを考えると，今回認められた血清中フェンタニル濃度の日内変動はこれらを含む複数の要因により生じている可能性が推察された。

尿中排泄について，フェンタニル，各代謝物およびそれらの総量の尿中累積排泄率は用量によらずほぼ一定であったことから，代謝パターンも用量により変化せず一定であると考えられた。また，尿中の主代謝物はノルフェンタニルであり，*p*-水酸化フェンタニルは抱合体として尿中に排泄されており，尿中代謝物の組成は24時間貼付時と同様の傾向を示していた。

HFT-290を72時間単回貼付したときの剥離後の製剤中に残存するフェンタニルクエン酸塩量から算出した吸収率は約70～80%であり，用量によらずほぼ同程度であった。24時間単回貼付時の吸収率が約60～70%であったことを考えると，貼付後24時間以降は製剤からの吸収はわずかであり，貼付後24時間で製剤からの薬物放出はほぼ終了しているものと推察された。このことは72時間貼付時の血清中フェンタニル濃度が貼付後24時間以降に低下がみられていることとも一致していると考えられる。

HFT-290を3日に1回反復貼付した際にも，貼り替え後24時間から72時間にかけて血清中フェンタニル濃度が低下する傾向がみられた。また，72時間単回貼付成績から予測される血清中フェンタニル濃度（重ね合わせ法によるシミュレーション値）と72時間反復貼付時の実測値はよく一致していることが確認され，反復貼付時の剥離後の製剤中の残存率より算出した吸収率は単回貼付時の吸収率と同程度であったことから，反復貼付による薬物動態的な変化はほとんどないものと考えられた。

既存のリザーバータイプのフェンタニル経皮吸収型製剤（フェンタニルとして2.5mg）を3日に1回貼付したときの血清中フェンタニル濃度はHFT-290（フェンタニルクエン酸塩として2 mg）を1日1回貼付したときの血清中フェンタニル濃度に近似していた。この結果から，HFT-290は既存のリザーバータイプのフェンタニル経皮吸収型製剤と同程度の治療効果が期待できるものと考えられた。

以上の結果から，安定した血清中フェンタニル濃度を得るという観点からはHFT-290を3日に1回貼付するよりも1日1回貼付の用法にすることが好ましいと考えられた。また，製剤からの吸収率は高く，HFT-290の反復貼付において血清中フェンタニル濃度に蓄積性はみられなかったことから，良好な薬物動態特性を示しているものと考えられた。がん疼痛患者を対象としたHFT-290の臨床第Ⅱ相および臨床第Ⅲ相試験において1日1回貼付で有効性，安全性が確認されていることから[18)19)]，HFT-290は患者の状態に応じ貼り替え時に貼付用量を調節でき（増量は2日ごと），安定した疼痛コントロールを得ることができる新しいフェンタニルクエン酸塩含有経皮吸収型製剤となることが期待される。

文　献

1）世界保健機関編集：がんの痛みからの解放－WHO方式がん疼痛治療法－．In：武田文和訳．第2版，金原出版，1996.

2）Paix A, Coleman A, Lees J, et al.：Subcutaneous fentanyl and sufentanil infusion substitution for morphine intolerance in cancer pain management. Pain, 63：263-9, 1995.

3）Hanks GW, Conno F, Cherny N, et al.：Morphine and alternative opioids in cancer pain：the EAPC recommendations. Br J Cancer, 84：587-93, 2001.

4）Kuhlman JJ Jr, McCaulley R, Valouch TJ, et al.：

Fentanyl use, misuse, and abuse : a summary of 23 postmortem cases. J Anal Toxicol, 27 : 499-504, 2003.

5) 松澤美香：新たな経皮吸収型オピオイド製剤の開発～デュロテップMTパッチ. BIO Clinica, 23 : 454-9, 2008.

6) 二村昭彦, 東口高志：がん疼痛治療におけるレスキュードーズ. 医薬ジャーナル, 44 : 142-8, 2008.

7) 沼田千賀子, 寺岡麗子, 松田芳久, 他：使用済みフェンタニルパッチ内のフェンタニル残存量の測定および残存率に影響を及ぼす要因－個人差および貼付部位－. 医療薬学, 31 : 599-605, 2005.

8) 太田孝一：臨床編3モルヒネ以外のオピオイド製剤とその特徴. In：並木昭義, 表圭一, 編集. オピオイド, 克誠堂出版, 75-89, 2005.

9) Kokubun H, Matoba M, Hoka S, et al. : Relationship between serum fentanyl concentration and transdermal fentanyl dosage, and intra-individual variability in fentanyl concentration after application of fentanyl patches in patients with cancer pain. 医療薬学, 33 : 200-5, 2007.

10) Tateishi T, Krivoruk Y, Ueng Y-F, et al. : Identification of human liver cytochrome P-450 3A4 as the enzime responsible for fentanyl and sufentanil N-dealkylation. Anesth Analg, 82 : 167-72, 1996.

11) Feierman D, Lasker J : Metabolism of fentanyl, a synthetic opioid analgesic, by human liver microsomes. Role of CYP3A4. Drug Metab Dispos, 24 : 932-9, 1996.

12) Shimada T, Yamazaki H, Mimura M, et al. : Interindividual variations in human liver cytochrome P-450 enzymes involved in the oxidation of drugs, carcinogens and toxic chemicals : studies with liver microsomes of 30 Japanese and 30 Caucasians. J Pharmacol Exp Ther, 270 : 414-23, 1994.

13) Varvel J, Shafer S, Hwang S, et al. : Absorption characteristics of transdermally administered fentanyl. Anesthesiology, 70 : 928-34, 1989.

14) 菅原幸子, 長谷川節男, 長沼英夫, 他：ロキソプロフェンナトリウム含有水性貼付剤（LX-A）の1日1回および1日2回5日間反復貼付時の薬物動態の検討. 臨床医薬, 22 : 279-92, 2006.

15) Yosipovitch G, Xiong G, Haus E, et al. : Time-dependent variations of the skin barrier function in humans : transepidermal water loss, stratum corneum hydration, skin surface pH, and skin temperature. J Invest Dermatol, 110 : 20-3, 1998.

16) Bruguerolle B : Chronopharmacokinetics. Clin Pharmacokinet, 35 : 83-94, 1998.

17) Ashburn M, Ogden L, Zhang J, et al. : The pharmacokinetics of transdermal fentanyl delivered with and without controlled heat. J Pain, 4 : 291-7, 2003.

18) 宮崎東洋, 並木昭義, 小川節郎, 他：がん疼痛に対する1日1回フェンタニルクエン酸塩貼付剤の第Ⅱ相臨床試験－リザーバー型フェンタニルパッチからの切り替え貼付－. 未発表（投稿準備中）.

19) 宮崎東洋, 並木昭義, 小川節郎, 他：がん疼痛に対するHFT-290の第Ⅲ相臨床試験－用量換算検証試験－. 未発表（投稿準備中）.

別紙４

研究成果の刊行に関する一覧表

書籍

著者氏名	論文タイトル名	書籍全体の編集者名	書　籍　名	出版社名	出版地	出版年	ページ

雑誌

発表者氏名	論文タイトル名	発表誌名	巻号	ページ	出版年
Minami K, Sudo Y, Shiraishi S, Seo M, Uezono Y.	The analysis of the effects of anesthesics and ethanol on m-opioid receptors.	J Pharmacol. Sci, 112		424-431	2010
Miyano K, Moriok a N, Sugimoto T, Shiraiashi S, Uezono Y, Nakata Y.	Activation of the neurokinin-1 receptor in rat spinal astrocytes induces Ca^{2+} release from IP_3-sensitive Ca^{2+} stores and extracellular Ca^{2+} influx through TRPC3.	Neurochem Int, 57		923-934	2010
Ando Y, Hojo M, Kanaide M, Takada M, Sudo Y, Shiraishi S, Sumikawa K, Uezono	Y. S(+)-Ketaminesuppresses desensitization of γ-aminobutyric acid type B receptor- mediated signaling by inhibition of the interaction of γ-aminobutyric acid type B receptors with G protein-coupled receptor kinase 4 or 5.	Anesthesiology	114	401-411	2011
白石成二	ストレスと副腎髄質と麻酔	Anesthesia Century 21	12	4-10	2010

J Pharmacol Sci 112, 424 - 431 (2010)

Journal of Pharmacological Sciences

Full Paper

Analysis of the Effects of Anesthetics and Ethanol on μ-Opioid Receptor

Kouichiro Minami[1,3,*], Yuka Sudo[2,3], Seiji Shiraishi[3], Masanori Seo[1], and Yasuhito Uezono[3]

[1]*Department of Anesthesiology and Critical Care Medicine, Jichi Medical University, Tochigi 329-0483, Japan*
[2]*Department of Molecular and Cellular Biology, Nagasaki University School of Biomedical Sciences, Nagasaki 852-8523, Japan*
[3]*Cancer Pathophysiology Division, National Cancer Center Research Institute, Tokyo 104-0045, Japan*

Received January 6, 2010; Accepted February 15, 2010

Abstract. G protein–coupled receptors, in particular, Ca^{2+}-mobilizing G_q-coupled receptors have been reported to be targets for anesthetics. Opioids are commonly used analgesics in clinical practice, but the effects of anesthetics on the opioid μ-receptors (μOR) have not been systematically examined. We report here an electrophysiological assay to analyze the effects of anesthetics and ethanol on the functions of μOR in *Xenopus* oocytes expressing a μOR fused to chimeric Gα protein G_{qi5} (μOR-G_{qi5}). Using this system, the effects of halothane, ketamine, propofol, and ethanol on the μOR functions were analyzed. In oocytes expressing μOR-G_{qi5}, the μOR agonist DAMGO ([D-Ala^2,*N*-MePhe^4,Gly-ol]-enkephalin) elicited Ca^{2+}-activated Cl^- currents in a concentration-dependent manner (EC_{50} = 0.24 μM). Ketamine, propofol, halothane, and ethanol themselves did not elicit any currents in oocytes expressing μOR-G_{qi5}, whereas ketamine and ethanol inhibited the DAMGO-induced Cl^- currents at clinically equivalent concentrations. Propofol and halothane inhibited the DAMGO-induced currents only at higher concentrations. These findings suggest that ketamine and ethanol may inhibit μOR functions in clinical practice. We propose that the electrophysiological assay in *Xenopus* oocytes expressing μOR-G_{qi5} would be useful for analyzing the effects of anesthetics and analgesics on opioid receptor function.

Keywords: μ-opioid receptor, $G_{i/o}$-coupled receptor, ketamine, ethanol, *Xenopus* oocyte

Introduction

Opioids are commonly used analgesics in clinical practice, but the role of opioid receptor (OR) in anesthetic action has still been unclear. It has been reported that the OR antagonist naloxone does not affect the anesthetic potency of volatile anesthetics halothane in animals (1, 2). On the other hand, Sarton et al. reported that S(+) ketamine interacts with the μ-opioid system at supraspinal sites (3). In order to clarify the role of ORs in anesthetic action, it would be necessary to study the direct effects on OR function.

Several lines of studies have been reported that metabotropic G protein–coupled receptors (GPCRs) are now recognized as targets for anesthetics and analgesics (4). We and others have previously reported that functions of G_q protein–coupled receptors, including muscarinic type1 receptors (M_1R) (5), metabotropic type 5 glutamate receptors (mGluR5) (6), 5-hydroxytryptamine (5HT) type 2A receptors (7), and substance P receptors (8), are inhibited by anesthetics and analgesics. The ORs belong to the GPCR family and three types of ORs, μ, δ, and κ, have been identified by molecular cloning (9). Within three subtypes of these receptors, μORs are the major receptor to mediate the analgesic effects of opioids (9). On the basis of second messenger signaling, μOR couple to $G\alpha_{i/o}$ protein to cause inhibition of adenylate cyclase, inhibition of voltage-dependent Ca^{2+} channels, or activation of G protein–coupled inwardly rectifying K^+ channels (GIRKs) (9). Functions of G_q-coupled receptors have been reported to be modified by some anesthetics and analgesics (4, 10); as far as the functions of $G_{i/o}$-coupled receptors including μOR are concerned, much less is known about the direct effects of anesthetics and analgesics.

The *Xenopus* oocyte expression system has widely

*Corresponding author. kminami@med.uoeh-u.ac.jp
Published online in J-STAGE on April 2, 2010 (in advance)
doi: 10.1254/jphs.10003FP

been employed to study functions of a number of GPCRs (4, 10). In the case of G_q-coupled receptors, stimulation of the receptors result in activation of Ca^{2+}-activated Cl^- currents in *Xenopus* oocytes by G_q-mediated activation of phospholipase C (PLC) and subsequent formation of IP_3 and diacylglycerol (4, 11). The IP_3 formed causes release of Ca^{2+} from the endoplasmic reticulum by activation of IP_3 receptors (IP_3R), which in turn, triggers the opening of Ca^{2+}-activated Cl^- channels endogenously expressed in the oocytes (4, 11). However, in the case of $G_{i/o}$-coupled receptors, analysis has been difficult due to lack of appropriate analytical output in oocytes. We have established the assay method for $G_{i/o}$-coupled receptors by using G_{qi5} chimeric G protein to switch the $G_{i/o}$ signal to a G_q signal (12). By using this assay system, we reported that halothane inhibited the function of $G_{i/o}$-coupled muscarinic M_2 receptor (M_2R) in oocytes coexpressing M_2R and G_{qi5} (13). Recently, in order to improve the $G_{i/o}$-coupled–receptor assay system, we made a μOR fused to G_{qi5} (μOR-G_{qi5}) and expressed it in *Xenopus* oocytes (13).

By using this assay system, we examined the effects of halothane, ketamine, propofol, and ethanol on the function of μOR.

Materials and Methods

Materials

Adult *Xenopus laevis* female frogs were purchased from Kato Kagaku (Tokyo); halothane, from Dinabot Laboratories (Osaka), and the Ultracomp *E. coli* Transformation Kit, from Invitrogen (San Diego, CA, USA). Purification of cDNAs was performed with a Qiagen purification kit (Qiagen, Chatworth, CA, USA). Gentamicin, sodium pyruvate, [D-Ala^2,*N*-MePhe^4,Gly-ol]-enkephalin (DAMGO), and propofol were purchased from Tokyo Kagaku (Tokyo), and ketamine was purchased from Sigma (St. Louis, MO, USA). Other chemicals are analytical grade and were from Nacalai Tesque (Kyoto). The rat μOR was provided by Dr. N. Dascal (Tel Aviv University, Ramat Aviv, Israel). The chimeric $G\alpha_{qi5}$ was a kind gift from Dr. B.R. Conklin (The University of California, San Francisco, CA, USA). Each of the cRNAs was prepared by using an mCAP mRNA Capping Kit and transcribed with a T7 RNA Polymerase in vitro Transcription Kit (Stratagene, La Jolla, CA, USA).

Preperartion of chimeric μOR-Gqi5

The tandem cDNAs of chimeric μOR-G_{qi5} was created by ligating the receptor cDNA sequences into the NheI site of G_{qi5} cDNAs. The sequences of all PCR products were confirmed by sequencing with ABI3100 (Applied BioSystems, Tokyo). All cDNAs for the synthesis of cRNAs were subcloned into the pGEMHJ vector, which provides the 5′- and 3′-untranslated region of the *Xenopus* β-globin RNA (14), ensuring a high level of protein expression in the oocytes. Each of the cRNAs was synthesized using the mCAP mRNA Capping Kit, with the T7 RNA polymerase in vitro Transcription Kit (Ambion, Austin, TX, USA) from the respective linearized cDNAs.

Recording and data analyses

Isolation and microinjection of *Xenopus* oocytes were performed as previously described (12, 13). *Xenopus* oocytes were injected with appropriate amounts of cRNAs (50 ng, μOR-G_{qi5}) and incubated with ND 96 medium composed of 96 mM NaCl, 2 mM KCl, 1.8 mM $CaCl_2$, 1 mM $MgCl_2$, 5 mM HEPES (pH 7.4, adjusted with NaOH), supplemented with 2.5 mM sodium pyruvate and 50 μg/ml gentamicin for 3 – 7 days until recording. Oocytes were placed in a 100-ml recording chamber and perfused with MBS (modified Barth's saline) composed of 88 mM NaCl, 1 mM KCl, 2.4 mM $NaHCO_3$, 10 mM HEPES, 0.82 mM $MgSO_4$, 0.33 mM $Ca(NO_3)_2$, and 0.91 mM $CaCl_2$, (pH 7.4 adjusted with NaOH) at a rate of 1.8 ml/min at room temperature. Recording and clamping electrodes (1 – 2 MΩ) were pulled from 1.2-mm outside diameter capillary tubing and filled with 3 M KCl. A recording electrode was imbedded in the animal's pole of oocytes, and once the resting membrane potential stabilized, a clamping electrode was inserted and the resting membrane potential was allowed to restabilize. A Warner OC 725-B oocyte clamp (Hampden, CT, USA) was used to voltage-clamp each oocyte at −70 mV. We analyzed the peak component of the transient inward currents induced by receptor agonists because this component is dependent on the concentrations of the receptor agonist applied and is quite reproducible, as described by Minami et al. (15). Anesthetics (halothane, ketamine, propofol) and ethanol were applied for 2 min before and during the application of test compounds to allow complete equilibration in the bath. The solutions of halothane were freshly prepared immediately before use. We calculated the final concentration of halothane in the recording chamber as reported previously (16), and accordingly, the concentrations of halothane represent the bath concentrations.

Statistical analyses

Results are expressed as percentages of control responses. The control responses were measured before and after each drug application, to take into account possible shifts in the control currents as recording proceeded. The "n" values refer to the number of oocytes studied. Each experiment was carried out with oocytes from at

least two different frogs. Statistical analyses were performed using a one-way ANOVA (analysis of variance) and the Dunnet correction. Curve fitting and estimation of EC_{50} values for the concentration–response curves were performed using Graphpad Inplot Software (San Diego, CA, USA).

Results

DAMGO-induced Ca^{2+}-activated Cl^- currents in Xenopus oocytes expressing μOR-G_{qi5}

We first determined the effects of the μOR agonist DAMGO on the Ca^{2+}-activated Cl^- currents in *Xenopus* oocytes expressing μOR-G_{qi5}. As shown in Fig. 1A, DAMGO at 0.1 μM elicited a robust Ca^{2+}-activated Cl^- current. There were no Cl^--currents in oocytes expressing μOR not fused to G_{qi5} even at 10 μM DAMGO (data not shown), as reported previously (13). The EC_{50} of the DAMGO-induced Cl^- currents was 0.24 ± 0.01 μM (Fig. 1B).

Analysis of ketamine and propofol on DAMGO-induced Ca^{2+}-activated Cl^- currents in Xenopus oocytes expressing μOR-G_{qi5}

By using this assay, we examined the effects of the intravenous anesthetic ketamine on the μOR function in *Xenopus* oocytes expressing μOR-G_{qi5}. Ketamine by itself did not elicit any currents in oocytes expressing μOR-G_{qi5} but significantly inhibited DAMGO-induced Ca^{2+}-activated Cl^- currents in a concentration-dependent manner (Fig. 2A). Ketamine at 0.1, 1, and 10 μM inhibited the

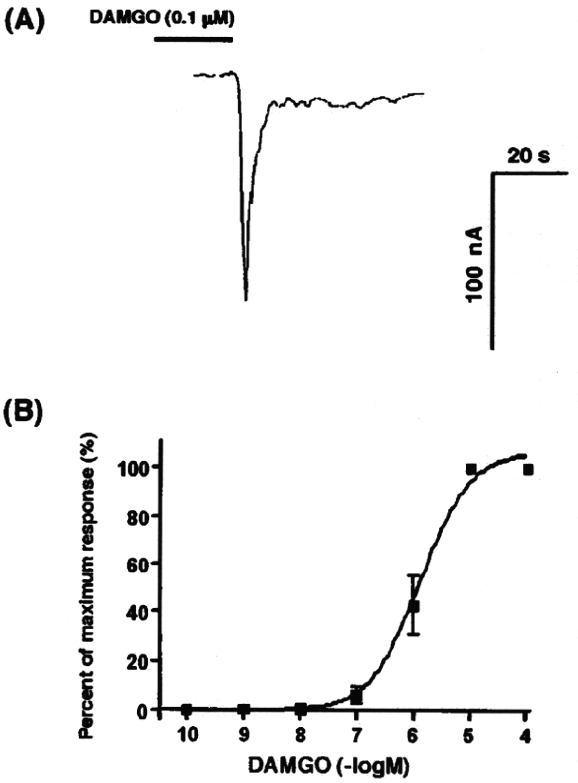

Fig. 1. Electrophysiological μOR assay induced by the μOR agonist DAMGO in *Xenopus* oocytes expressing μOR-G_{qi5}. A: Typical tracing of DAMGO (0.1 μM)-induced Ca^{2+}-activaed Cl^- current in an oocyte expressing μOR-G_{qi5}. B: Concentration–response curves of DAMGO-induced Ca^{2+}-activated Cl^- currents in oocytes. Oocytes were voltage-clamped at −70 mV and DAMGO was applied for 20 s.

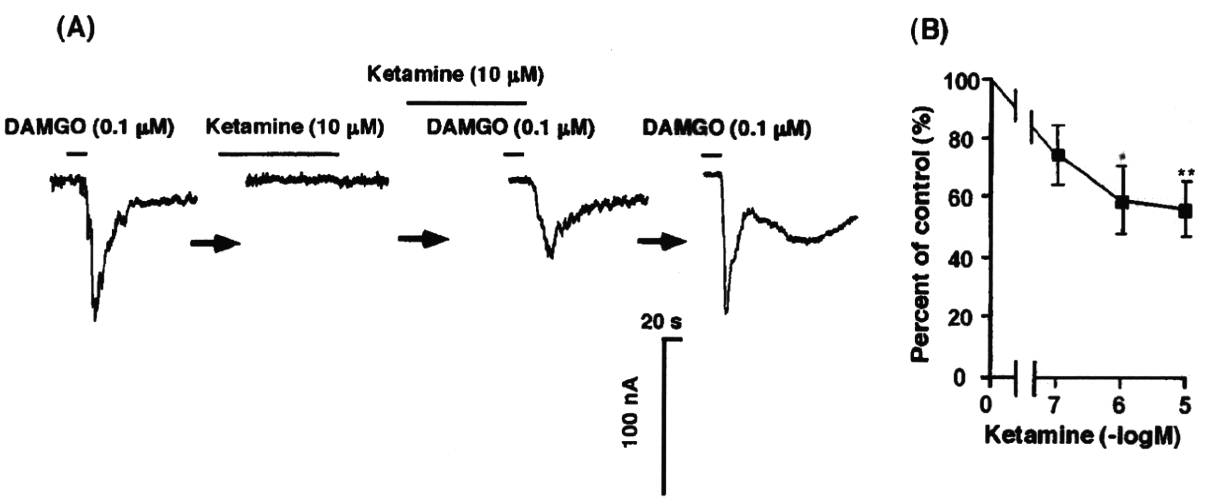

Fig. 2. Effects of ketamine on the basal and DAMGO-induced Ca^{2+}-activated Cl^- currents in oocytes expressing μOR-G_{qi5}. A: Typical tracings of the effect of 10 μM ketamine on the Cl^- current evoked by 0.1 μM DAMGO in an oocyte expressing μOR-G_{qi5}. B: Concentration–response curve for the inhibitory effects of ketamine on DAMGO (0.1 μM)-induced Cl^- currents in oocytes expressing μOR-G_{qi5}. $^*P < 0.05$ and $^{**}P < 0.01$ vs. control.

DAMGO-induced Cl^- currents to 74 ± 10.3%, 59.1 ± 11.3%, and 56.2 ± 9.3% of the control value, respectively (n = 6 for each) (Fig. 2B).

We next determined the effects of another intravenous anesthetic propofol on the function of μOR in oocytes expressing μOR-G_{qi5} (Fig. 3). Propofol by itself elicited no currents, but inhibited DAMGO-induced Cl^- currents in oocytes expressing μOR-G_{qi5} in a concentration-dependent manner (Fig. 3A). Propofol at concentrations of 0.1, 1, 10, and 100 μM inhibited the DAMGO-induced Cl^- currents to 93.3 ± 3.7%, 73.5 ± 7.9%, 72.8 ± 5.7%, and 53.7 ± 7.5% of the control value, respectively (n = 6 for each) (Fig. 3B).

Analysis of halothane and ethanol on the DAMGO-induced Ca^{2+}-activated Cl^- currents in Xenopus oocytes expressing μOR-G_{qi5}

We then examined the effects of the volatile anesthetic halothane on the function of μOR in oocytes expressing μOR-G_{qi5} (Fig. 4). Halothane by itself did not elicit any currents in oocytes expressing μOR-G_{qi5} at concentrations up to 2 mM, (Fig. 4A). Higher concentrations of halothane more than 1 minimum alveolar concentration (MAC, 0.25 mM) had inhibitory effects on the DAMGO-induced Cl^- currents in a concentration-dependent manner; 1MAC concentration of halothane did not suppress DAMGO-induced Cl^- currents. Halothane at concentrations of 0.25, 0.5, 1, and 2 mM inhibited the current to 75.1 ± 12.4%, 57.8 ± 10.3%, 54.7 ± 10.3%, and 48.6 ± 9.4% of the control value, respectively (n = 6 for each) (Fig. 4B).

We finally examined the effects of ethanol on the function of μOR in oocytes expressing μOR-G_{qi5} (Fig. 5). Ethanol by itself had no effects in oocytes expressing μOR-G_{qi5}, but it significantly inhibited DAMGO-induced Cl^- currents in a concentration-dependent manner (Fig. 5B). Ethanol at concentrations of 25, 50, 100, and 200 mM inhibited the currents to 53.1 ± 10.1%, 47 ± 13.3%, 43.3 ± 9.6%, and 35 ± 5.3% of the control value, respectively (n = 6 for each) (Fig. 5B).

Discussion

We previously proposed an electrophysiological assay of the $G_{i/o}$-coupled receptors in *Xenopus* oocytes expressing the receptors and chimeric G protein G_{qi5} (12, 13). By using this system, we examined the effects of several anesthetics and ethanol on the μOR function in oocytes expressing fused μOR-G_{qi5}.

In general, $G_{i/o}$-coupled receptors such as μOR are known to inhibit adenylate cyclase to decrease cAMP levels in the cells (9). Numerous reports have shown that ketamine, halothane, and ethanol increase basal cAMP levels in a variety of the cells, possibly by direct activation of adenylate cyclases (17 – 20); thus it might be difficult to estimate the effects of anesthetics and ethanol

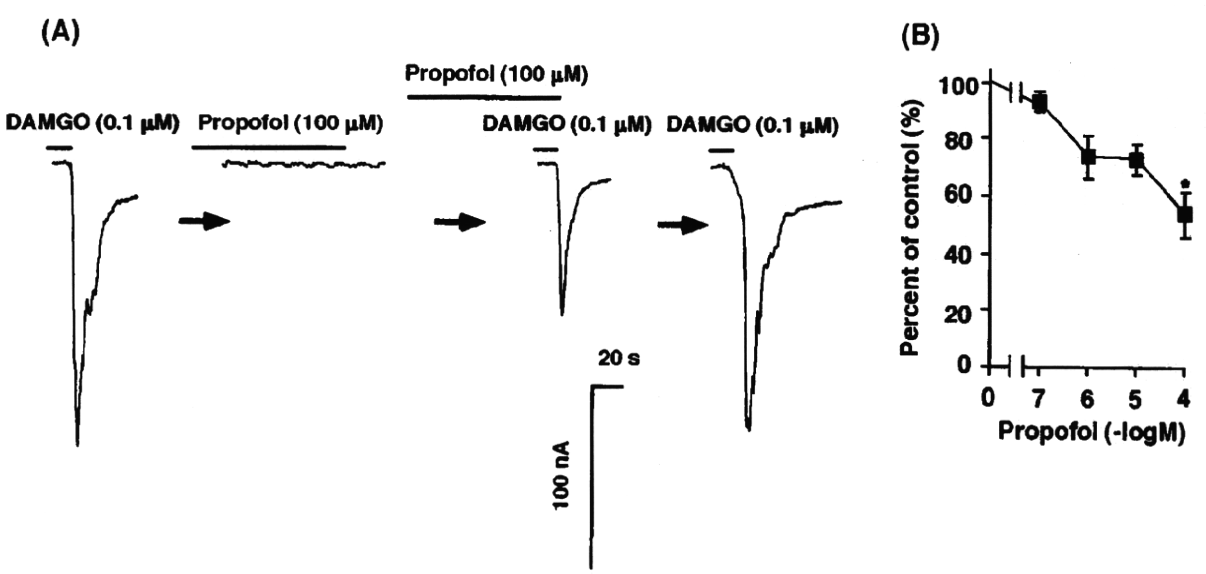

Fig. 3. Effects of propofol on the basal and DAMGO-induced Ca^{2+}-activated Cl^- currents in oocytes expressing μOR-G_{qi5}. A: Typical tracings of the effect of 100 μM propofol on the Cl^- current evoked by 0.1 μM DAMGO in an oocyte expressing μOR-G_{qi5}. B: Concentration–response curve for the inhibitory effects of propofol on DAMGO (0.1 μM)–induced Cl^- currents in oocytes expressing μOR-G_{qi5} *$P < 0.05$ and vs. control.

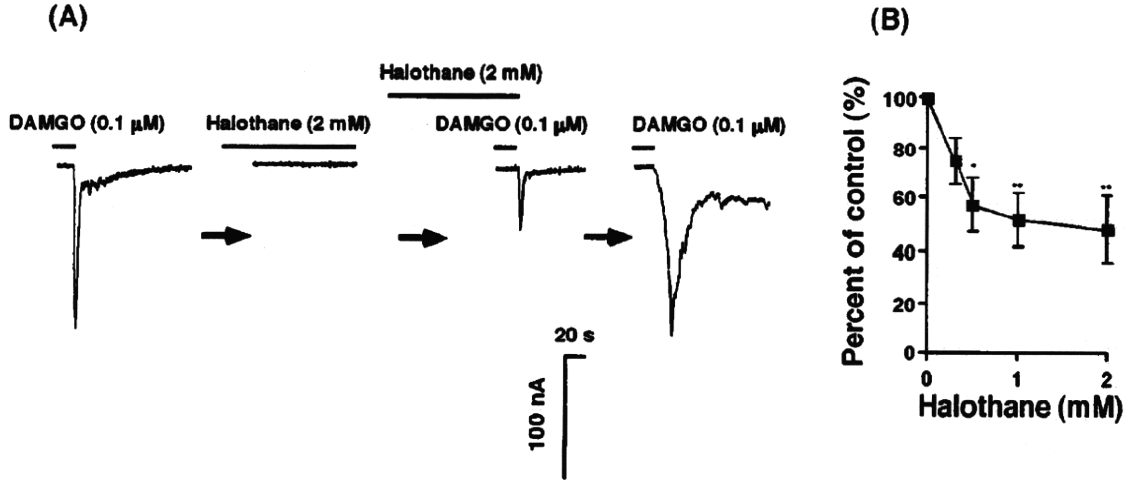

Fig. 4. Effects of halothane on the basal and DAMGO-induced Ca^{2+}-activated Cl^- currents in oocytes expressing μOR-G_{qi5}. A: Typical tracings of the effect of 2 mM halothane on the Cl^- current evoked by 0.1 μM DAMGO in an oocyte expressing μOR-G_{qi5}. B: Concentration–response curve for the inhibitory effects of halothane on DAMGO (0.1 μM)–induced Cl^- currents in oocytes expressing μOR-G_{qi5}. $^*P < 0.05$ and $^{**}P < 0.01$ vs. control.

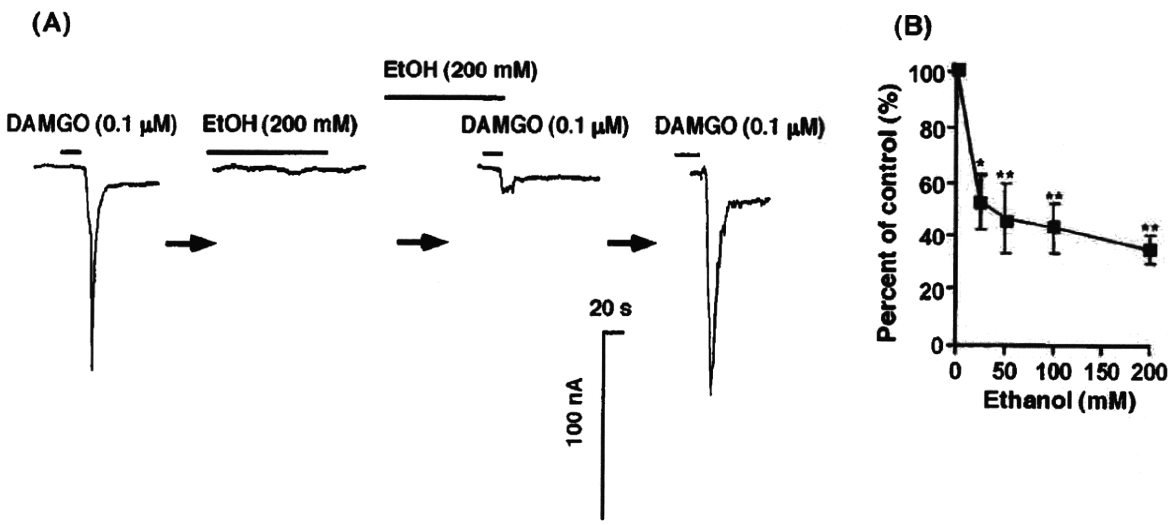

Fig. 5. Effects of ethanol on the basal and DAMGO-induced Ca^{2+}-activated Cl^- currents in oocytes expressing μOR-G_{qi5}. A: Typical tracings of the effect of 200 mM ethanol on the Cl^- current evoked by 0.1 μM DAMGO in an oocyte expressing μOR-G_{qi5}. B: Concentration–response curve for the inhibitory effects of ethanol on DAMGO (0.1 μM)–induced Cl^- currents in oocytes expressing μOR-G_{qi5}. $^*P < 0.05$ and $^{**}P < 0.01$ vs. control.

on the functions of $G_{i/o}$-coupled receptors by using a cAMP inhibition assay. Alternatively we and others have used *Xenopus* oocytes expressing GIRK channels for the analysis of functions of $G_{i/o}$-coupled receptors such as μOR, $GABA_BR$, or cannabinoid CB_1 and CB_2 receptors (13, 21 – 23); GIRKs have been demonstrated to be excellent reporter channels for assay of the activity of $G_{i/o}$-coupled receptors (21). However, recent reports have revealed that GIRKs are possible targets for several anesthetics including halothane and ethanol (24 – 26). In such a situation, it should be taken into consideration that functions of either $G_{i/o}$-coupled receptors, GIRKs, or both could be affected by anesthetics or alcohol if GIRKs are used as reporters (24 – 26). In this study, we thus employed μOR-G_{qi5} in a *Xenopus* oocyte expression assay system. Accordingly, this system makes it possible

to study the direct effects of anesthetics and alcohols on μOR functions.

In the present study, we demonstrated that ketamine and ethanol inhibited the DAMGO-induced Cl^- currents at clinically equivalent concentrations, while propofol and halothane inhibited the DAMGO-induced currents only at higher concentrations. In our experimental system, the inhibitory effects of the anesthetics and ethanol are considered due to specific inhibition of μOR or the inhibition of the downstream steps in the μOR-induced G_{qi5}–PLC–IP_3–IP_3R–Ca^{2+} mobilization pathways. There are numerous reports showing that ketamine, propofol, halothane, and ethanol did not inhibit such downstream pathways after activation of GPCRs in the *Xenopus* oocyte expression system. In the case of ketamine and halothane, they inhibit muscarinic M_1R-mediated Ca^{2+}-activated Cl^- currents in clinically relevant concentrations (5, 27) without affecting angiotensin II receptor (AT_1R)–induced Cl^- currents, although activation of M_1R and AT_1R consequently activate the same G_q–PLC–IP_3–IP_3R–Ca^{2+} mobilization pathways (5, 27). These results suggest that ketamine and halothane affect functions of Ca^{2+}-mobilizing GPCRs possibly by receptor sites rather than the downstream pathway after GPCR activation. As for propofol, our previous study demonstrated that this anesthetic inhibited the functions of M_1R but not substance P receptors, although both receptors were considered to couple to the same Gq-mediated pathways (8, 28). In addition, we demonstrated that propofol (50 μM) did not inhibit the direct G protein activator AlF_4^-–induced Ca^{2+}-activated Cl^- currents in *Xenopus* oocytes (28). In the case of ethanol, we previously reported that ethanol also selectively inhibited the glutamate mGluR5 but not mGluR1, although both receptors couple to Gq to activate Ca^{2+}-activated Cl^- currents in oocytes (6). Taken together, these findings indicate that anesthetics and ethanol employed in the present study may not inhibit the step of G protein–PLC–IP_3–IP_3R–Ca^{2+} mobilization in the μOR signaling pathway.

The EC_{50} value of DAMGO of the μOR-induced Ca^{2+}-activated Cl^--currents through G_{qi5} was 0.24 μM in the present study. In our previous experimental study in *Xenopus* oocytes expressing μOR-G_{qi5} (13), the EC_{50} of DAMGO was approximately 0.1 μM. In *Xenopus* oocytes expressing cloned μOR and GIRKs, the EC_{50} values of DAMGO were 0.1 (13), 0.034 – 0.133 (29), and 0.02 – 0.09 μM (30) determined with the GIRK channel assay. These results suggest that our present EC_{50} value seems not too far from the previously reported EC_{50} values obtained in *Xenopus* oocytes expressing μOR.

We showed that ketamine had an inhibitory effect on DAMGO-induced Cl^- currents in oocytes expressing μOR-G_{qi5} at concentrations more than 1 μM. In clinical situations, the free plasma concentration of ketamine was approximately 10.5 – 60 μM (31, 32). Previous reports showed that higher concentration of ketamine than those in clinical usage (50 – 100 μM) displaced [^{3}H]diprenorphine binding to μORs expressed in Chinese hamster ovary cells (33). In an animal study, S(+)ketamine interacts with the μOR, which contributed to S(+)ketamine-induced respiratory depression and supraspinal antinociception (3). Consistent with these reports, our present results suggest that anesthetic concentrations of ketamine would have direct inhibitory effects on μOR.

The effects of propofol on the μOR functions have not been reported so far. In the present study, only high concentration (100 μM) of propofol (but less than 100 μM) had inhibitory effects on the DAMGO-induced Cl^- currents in oocytes expressing μOR-G_{qi5}. In humans, the peak plasma concentration of propofol after intravenous injection of the anesthetic dosage of 2.5 mg/kg was approximately 23 ± 0.24 μM (34). From our present results, it seems that propofol would have little effect on the μOR functions in its clinically used concentrations.

The direct effects of halothane on the μOR have not been studied. In the present study, clinical concentrations of halothane (0.25 mM) had no effect on basal- and DAMGO-induced Cl^- currents in *Xenopus* oocytes expressing μOR-G_{qi5}, whereas higher concentrations of halothane (0.5 – 2.0 mM) inhibited the DAMGO-induced Cl^- currents. To our knowledge, this is the first report that shows the direct effects of halothane on the function of μOR in the heterologous expression system. Lambert et al. have reported that binding of [^{3}H]DAMGO was unaffected by lower concentrations of halothane, but 5.0% (approximately 5.3 MAC) halothane reduced its affinity (35). From our present and previous reports, higher concentrations of halothane would inhibit the DAMGO-induced currents by reducing the affinity of DAMGO to μOR. Yamakura et al., on the other hand, reported that inhibition by halothane is likely caused by inhibition of GIRK channels, not by μOR (25). Furthermore, it was recently reported that the MACs for halothane are not different between wild-type and μOR-knock-out mice (36). Although further study would be necessary, our present result suggests that halothane would have little effect on μOR in the clinical situation.

Interaction between alcohol and the CNS opioid signaling system is well established in both basic and clinical research (37, 38). However, mechanisms involving direct ethanol interaction on the μOR have not been fully elucidated. We showed that ethanol at a concentration more than 25 mM inhibited DAMGO-induced Cl^- currents in oocytes expressing μOR-G_{qi5}. Several hypotheses of such inhibitory effects have been asserted; Vukojević et al. reported that relevant concentrations of ethanol

(10 – 40 mM) altered μOR mobility and surface density and affect the dynamics of plasma membrane lipids of pheochromocytoma PC12 cells, suggesting that ethanol modified μOR activity by sorting of μOR at the plasma membrane (39). Although further studies will be required, ethanol might inhibit the DAMGO-induced currents by reducing the affinity of DAMGO to the μOR.

In conclusion, we demonstrated that ketamine and ethanol have significant inhibitory effects on the function of μOR at clinically relevant concentrations. On the other hand, halothane and propofol seem not to suppress the μOR functions at least at clinically used concentrations. Further studies will be necessary to clarify the effects of these agents on opioid systems with other assay systems. The electrophysiological method for analysis of the function of μOR fused to the chimeric Gα protein shown in this study could be useful for investigating the effects of analgesics, anesthetics, and alcohol on other $G_{i/o}$-coupled receptors.

Acknowledgments

The authors would like to thank all the members in Cancer Pathophysiology Division in National Cancer Center Research Institute. This work was supported by grants from the Ministry of Education, Culture, Sports, Science, and Technology of Japan (K.M., Y.U.); Smoking foundation (Y.U., Y.S.); Foundation of Daiichi-Sankyo Pharmaceuticals (Y.U.); a Third Term Comprehensive 10-year Strategy for Cancer Control from the Japanese Ministry of Health, Labour and Welfare; and a Grant-in-Aid for Cancer Research from the Ministry of Health, Labour and Welfare of Japan.

References

1 Harper MH, Winter PM, Johnson BH, Eger EI 2nd. Naloxone does not antagonize general anesthesia in the rat. Anesthesiology. 1978;49:3–5.
2 Pace NL, Wong KC. Failure of naloxone and naltrexone to antagonize halothane anesthesia in the dog. Anesth Analg. 1979;58:36–39.
3 Sarton E, Teppema LJ, Olievier C, Nieuwenhuijs D, Matthes HW, Kieffer BL, et al. The involvement of the mu-opioid receptor in ketamine-induced respiratory depression and antinociception. Anesth Analg. 2001;93:1495–1500.
4 Minami K, Uezono Y. G_q protein-coupled receptors as targets for anesthetics. Curr Pharm Des. 2006;12:1931–1937.
5 Durieux ME. Muscarinic signaling in the central nervous system. Recent developments and anesthetic implications. Anesthesiology. 1996;84:173–189.
6 Minami K, Gereau RW 4th, Minami M, Heinemann SF, Harris RA. Effects of ethanol and anesthetics on type 1 and 5 metabotropic glutamate receptors expressed in *Xenopus* laevis oocytes. Mol Pharmacol. 1998;53:148–156.
7 Minami K, Minami M, Harris RA. Inhibition of 5-hydroxytryptamine type 2A receptor-induced currents by n-alcohols and anesthetics. J Pharmacol Exp Ther. 1997;281:1136–1143.
8 Okamoto T, Minami K, Uezono Y, Ogata J, Shiraishi M, Shigematsu A, et al. The inhibitory effects of ketamine and pentobarbital on substance P receptors expressed in *Xenopus* oocytes. Anesth Analg. 2003;97:104–110.
9 Surratt CK, Adams WR. G protein-coupled receptor structural motifs: relevance to the opioid receptors. Curr Top Med Chem. 2005;5:315–324.
10 Minami K, Uezono Y, Ueta Y. Pharmacological aspects of the effects of tramadol on G-protein coupled receptors. J Pharmacol Sci. 2007;103:253–260.
11 Dascal N. The use of *Xenopus* oocytes for the study of ion channels. CRC Crit Rev Biochem. 1987;22:317–387.
12 Minami K, Uezono Y, Shiraishi M, Okamoto T, Ogata J, Horishita T, et al. Analysis of the effects of halothane on G_i-coupled muscarinic M_2 receptor signaling in *Xenopus* oocytes using a chimeric Gα protein. Pharmacology. 2004;72:205–212.
13 Hojo M, Sudo Y, Ando Y, Minami K, Takada M, Matsubara T, et al. μ-Opioid receptor forms a functional heterodimer with cannabinoid CB_1 receptor: electrophysiological and FRET assay analysis. J Pharmacol Sci. 2008;108:308–319.
14 Vorobiov D, Bera AK, Keren-Raifman T, Barzilai R, Dascal N. Coupling of the muscarinic M_2 receptor to G protein-activated K^+ channels via $G\alpha_i$ and a receptor-$G\alpha_i$ fusion protein. Fusion between the receptor and $G\alpha_i$ eliminates catalytic (collision) coupling. J Biol Chem. 2000;275:4166–4170.
15 Minami K, Vanderah TW, Minami M, Harris RA. Inhibitory effects of anesthetics and ethanol on muscarinic receptors expressed in *Xenopus* oocytes. Eur J Pharmacol. 1997;339:237–244.
16 Dildy-Mayfield JE, Mihic SJ, Liu Y, Deitrich RA, Harris RA. Actions of long chain alcohols on GABAA and glutamate receptors: relation to in vivo effects. Br J Pharmacol. 1996;118:378–384.
17 Jimi N, Segawa K, Minami K, Sata T, SHigematsu A. Inhibitory effects of the intravenous anesthetic, ketamine, on rat mesangial cell proliferation. Anesth Analg. 1997;84:190–195
18 Bohm M, Schmidt U, Gieschik P, Schwinger RH, Bohm S, Erdmann E. Sensitization of adenylate cyclase by halothane in human myocardium and S49 lymphoma wild-type and cyc- cells: evidence for inactivation of the inhibitory G protein $G_i\alpha$. Mol Pharmacol. 1994;45:380–389.
19 Trimer L, Vulliemoz Y, Woo S-Y, Verosky M. Halotane effect on cAMP generation and hydrolysis in rat brain. Eur J Pharmacol. 1980;66:73–80.
20 Maas JW Jr, Vogt SK, Chan GCK, Pineda VV, Storm DR, Muglia LJ. Calcium-stimulated adenylate cyclase are critical modulators of neuronal ethanol sensitivity. J Neurosci. 2005;25:4118–4126.
21 Dascal N. Signalling via the G protein-activated K^+ channels. Cell Signal. 1997;9:551–573.
22 Uezono Y, Akihara M, Kaibara M, Kawano C, Shibuya I, Ueda Y, et al. Activation of inwardly rectifying K^+ channels by GABA-B receptors expressed in *Xenopus* oocytes. Neuroreport. 1998;9:583–587.
23 Ho BY, Uezono Y, Takada S, Takase I, Izumi F. Coupling of the expressed cannabinoid CB_1 and CB_2 receptors to phospholipase C and G protein-coupled inwardly rectifying K^+ channels. Receptors Channels. 1999;6:363–374.
24 Weigl LG, Schreibmayer W. G protein-gated inwardly rectifying potassium channels are targets for volatile anesthetics. Mol Pharmacol. 2001;60:282–289.
25 Yamakura T, Lewohl JM, Harris RA. Differential effects of general anesthetics on G protein-coupled inwardly rectifying and

other potassium channels. Anesthesiology. 2001;95:144–153.
26 Lewohl JM, Wilson WR, Mayfield RD, Brozowski SJ, Morrisett RA, Harris RA. G-protein-coupled inwardly rectifying potassium channels are targets of alcohol action. Nat Neurosci. 1999;2:1084–1090.
27 Inhibition by ketamine of muscarinic acetylcholine receptor function. Durieux ME. Anesth Analg. 1995;81:57–62.
28 Nagase Y, Kaibara M, Uezono Y, Izumi F, Sumikawa K, Taniyama K. Propofol inhibits muscarinic acetylcholine receptor-mediated signal transduction in *Xenopus* oocytes expressing the rat M_1 receptor. J Pharmacol Sci. 1999;79:319–325.
29 Kovoor A, Celver JP, Wu A, Chavkin C. Agonist induced homologous desensitization of μ-opioid receptors mediated by G protein-coupled receptor kinases is dependent on agonist efficacy. Mol Pharmacol. 1998;54:704–711.
30 Tyrosine phosphorylation of the μ-opioid receptor regulates agonist intrinsic efficacy. Mol Pharmacol. 2001;59:1360–1368.
31 Wieber J, Gugler R, Hengstmann JH, Dengler HJ. Pharmacokinetics of ketamine in man. Anaesthesist. 1975;24:260–263.
32 Idvall J, Ahlgren I, Aronsen KR, Stenberg P. Ketamine infusions: pharmacokinetics and clinical effects. Br J Anaesth. 1979;51:1167–1173.
33 Hirota K, Okawa H, Appadu BL, Grandy DK, Devi LA, Lambert DG. Stereoselective interaction of ketamine with recombinant mu, kappa, and delta opioid receptors expressed in Chinese hamster ovary cells. Anesthesiology. 1999;90:174–182.
34 Kirkpatrick T, Cockshott ID, Douglas EJ, Nimmo WS. Pharmacokinetics of propofol (diprivan) in elderly patients. Br J Anaesth. 1988;60:146–150.
35 Lambert DG, Appadu BL. Muscarinic receptor subtypes: do they have a place in clinical anaesthesia? Br J Anaesth. 1995;74:497–499.
36 Koyama T, Mayahara T, Wakamatsu T, Sora I, Fukuda K. Deletion of μ-opioid receptor in mice does not affect the minimum alveolar concentration of volatile anaesthetics and nitrous oxide-induced analgesia. Br J Anaesth. 2009;103:744–749.
37 Oswald LM, Wand GS. Opioids and alcoholism. Physiol Behav. 2004;81:339–358.
38 Herz A. Endogenous opioid systems and alcohol addiction. Psychopharmacology (Berl). 1997;129:99–111.
39 Vukojevic V, Ming Y, D'Addario C, Rigler R, Johansson B, Terenius L. Ethanol/naltrexone interactions at the mu-opioid receptor. CLSM/FCS study in live cells. PLoS One. 2008;3:e4008.

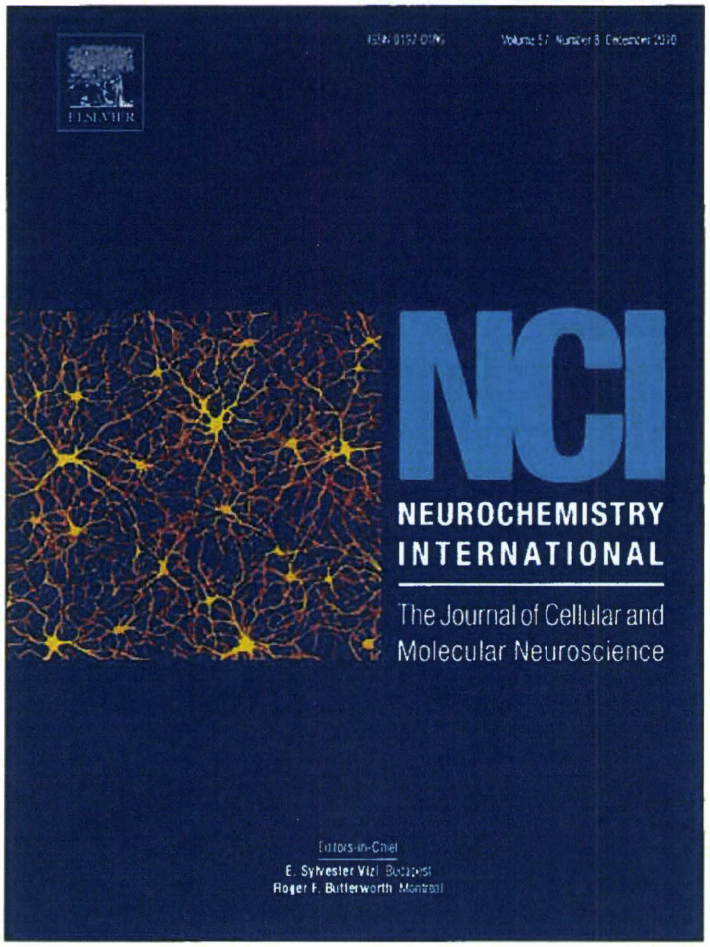

Neurochemistry International 57 (2010) 923–934

Contents lists available at ScienceDirect

Neurochemistry International

journal homepage: www.elsevier.com/locate/neuint

Activation of the neurokinin-1 receptor in rat spinal astrocytes induces Ca^{2+} release from IP_3-sensitive Ca^{2+} stores and extracellular Ca^{2+} influx through TRPC3

Kanako Miyano [a,b], Norimitsu Morioka [a,*], Tatsuhiko Sugimoto [a], Seiji Shiraishi [b], Yasuhito Uezono [b], Yoshihiro Nakata [a]

[a] Department of Pharmacology, Graduate School of Biomedical Sciences, Hiroshima University, Kasumi 1-2-3, Minami-ku, Hiroshima 734-8551, Japan
[b] Cancer Pathophysiology Division, National Cancer Center Research Institute, 5-1-1, Tsukiji, Chuo-ku, Tokyo 104-0045, Japan

ARTICLE INFO

Article history:
Received 1 July 2010
Received in revised form 9 September 2010
Accepted 20 September 2010
Available online 7 October 2010

Keywords:
Substance P
Spinal astrocyte
Neurokinin-1 receptor
TRPC3 channels
Protein kinase A
Protein kinase C

ABSTRACT

Substance P (SP) plays an important role in pain transmission through the stimulation of the neurokinin (NK) receptors expressed in neurons of the spinal cord, and the subsequent increase in the intracellular Ca^{2+} concentration ($[Ca^{2+}]_i$) as a result of this stimulation. Recent studies suggest that spinal astrocytes also contribute to SP-related pain transmission through the activation of NK receptors. However, the mechanisms involved in the SP-stimulated $[Ca^{2+}]_i$ increase by spinal astrocytes are unclear. We therefore examined whether (and how) the activation of NK receptors evoked increase in $[Ca^{2+}]_i$ in rat cultured spinal astrocytes using a Ca^{2+} imaging assay. Both SP and GR73632 (a selective agonist of the NK1 receptor) induced both transient and sustained increases in $[Ca^{2+}]_i$ in a dose-dependent manner. The SP-induced increase in $[Ca^{2+}]_i$ was significantly attenuated by CP-96345 (an NK1 receptor antagonist). The GR73632-induced increase in $[Ca^{2+}]_i$ was completely inhibited by pretreatment with U73122 (a phospholipase C inhibitor) or xestospongin C (an inositol 1,4,5-triphosphate (IP_3) receptor inhibitor). In the absence of extracellular Ca^{2+}, GR73632 induced only a transient increase in $[Ca^{2+}]_i$. In addition, H89, an inhibitor of protein kinase A (PKA), decreased the GR73632-mediated Ca^{2+} release from intracellular Ca^{2+} stores, while bisindolylmaleimide I, an inhibitor of protein kinase C (PKC), enhanced the GR73632-induced influx of extracellular Ca^{2+}. RT-PCR assays revealed that canonical transient receptor potential (TRPC) 1, 2, 3, 4 and 6 mRNA were expressed in spinal astrocytes. Moreover, BTP2 (a general TRPC channel inhibitor) or Pyr3 (a TRPC3 inhibitor) markedly blocked the GR73632-induced sustained increase in $[Ca^{2+}]_i$. These findings suggest that the stimulation of the NK-1 receptor in spinal astrocytes induces Ca^{2+} release from IP_3-sensitive intracellular Ca^{2+} stores, which is positively modulated by PKA, and subsequent Ca^{2+} influx through TRPC3, which is negatively regulated by PKC.

1. Introduction

Substance P (SP), a member of the tachykinin peptide family, is mainly expressed in primary afferent neurons (Severini et al., 2002). The centrally directed axonal terminals of SP-containing dorsal root ganglion (DRG) neurons project to the superficial lamina of the spinal horn, and their distally directed axonal terminals reside in peripheral tissues. In the spinal dorsal horn, SP released from the central terminals of primary afferent neurons by noxious stimuli activates the SP receptor, neurokinin (NK) receptor, which is expressed on the postsynaptic membrane, thus resulting in the transmission of nociceptive information to the central nervous system (Randic and Miletic, 1977; Hirota et al., 1985).

It is well known that SP binds to all subtypes of NK receptor; NK-1, -2 and -3 (Maggi, 1995). Among the three subtypes, SP has the highest affinity to NK-1 receptor (Maggi and Schwartz, 1997). The stimulation of NK receptors evokes the activation of phospholipase C (PLC), thus leading to phosphoinositol breakdown and an elevation of the intracellular Ca^{2+} concentration ($[Ca^{2+}]_i$) (Maggi, 1995; Snijdelaar et al., 2000). In addition, NK receptors also activate adenylate cyclase in order to induce cyclic AMP production (Nakajima et al., 1992; Maggi, 1995; Snijdelaar et al.,

Abbreviations: 2-APB, 2-aminoethyl diphenylborinate; BIM, bisindolylmaleimide I; BTP2, N-{4-[3,5-bis(trifluoromethyl)-1H-pyrazol-1-yl]phenyl}-4methyl-1,2,3-thiadiazole-5-carboxamide; $[Ca^{2+}]_i$, intracellular Ca^{2+} concentration; DAG, diacylglycerol; DMEM, Dulbecco's modified Eagle's medium; DRG, dorsal root ganglion; fura-2 AM, fura-2 acetoxymethyl ester; GFAP, glial fibrillary acidic protein; Hank's buffer, Hanks' balanced salt solution; IP_3, inositol 1,4,5-triphosphate; NK, neurokinin; PLC, phospholipase C; PKA, protein kinase A; PKC, protein kinase C; Pyr3, ethyl-1-(4-(2,3,3-trichloroacrylamide)phenyl)-5-(trifluoromethyl)-1H-pyrazole-4-carboxylate; SP, substance P; TRPC channel, canonical transient receptor potential channel.

* Corresponding author. Tel.: +81 82 257 5312; fax: +81 82 257 5314.
E-mail addresses: nmori@hiroshima-u.ac.jp, mnori@hiroshima-u.ac (N. Morioka).

0197-0186/$ – see front matter © 2010 Elsevier Ltd. All rights reserved.
doi:10.1016/j.neuint.2010.09.012

2000). Recent studies have shown that spinal astrocytes, the major population of glia supporting neurons, also express functional NK-1 receptor (Marriott et al., 1991; Palma et al., 1997). Therefore, SP released from the nerve terminal may act not only neurons, but also on the astrocytes surrounding synaptic junctions in the spinal cord. In this manner, SP may induce the increase of $[Ca^{2+}]_i$ via spinal astrocytes. This successive event has an important role in communication between neurons and astrocytes, and might be essential to achieve the synaptic transmission (Fields and Stevens-Graham, 2002). It is therefore possible that NK receptors on spinal astrocytes may also be associated with SP-related pain transmission. Although it has been showed that the activation of the NK-1 receptor on spinal astrocytes produces inositol 1,4,5-triposphate (IP_3) (Marriott et al., 1991; Palma et al., 1997), the Ca^{2+} signaling induced by the activation of that receptor in spinal astrocytes has not yet been investigated.

Recently, activation of the PLC-linked receptor (histamine receptor and proteinase-activated receptor) was reported to induce Ca^{2+} release from the intracellular Ca^{2+} stores through the IP_3 receptor, and also has been shown to cause the influx of extracellular Ca^{2+} in human astrocytoma (Barajas et al., 2008; Nakao et al., 2008). Several reports have demonstrated that the family of canonical transient receptor potential (TRPC) channels is one of candidate receptors responsible for mediating the extracellular Ca^{2+} influx induced after the activation of PLC-linked receptors in vasucular smooth muscle and TRPC channel-expressing cells (Venkatachalam and Montell, 2007; Large et al., 2009). Moreover, functional TRPC channels are also expressed in human astrocytoma (Barajas et al., 2008; Nakao et al., 2008). Therefore, these reports indicate the possibility that the NK-1 receptor-stimulated increase in $[Ca^{2+}]_i$ by spinal astrocytes involves the Ca^{2+} influx through TRPC channels. However, it is unclear whether the stimulation of the NK-1 receptor causes Ca^{2+} influx though TRPC channels in spinal astrocytes. The present study is the first to demonstrate that the activation of the NK-1 receptor by SP or GR73632, a selective NK-1 receptor agonist, evoked an increase in $[Ca^{2+}]_i$ in cultured spinal astrocytes, which involved both Ca^{2+} release from intracellular Ca^{2+} stores, and extracellular Ca^{2+} influx through the TRPC channels.

2. Materials and methods

2.1. Materials

The following drugs and reagents were used for the present studies: bisindolylmaleimide I (BIM) and N-{4-[3,5-bis(trifluoromethyl)-1H-pyrazol-1-yl]phenyl}-4methyl-1,2,3-thiadiazole-5-carboxamide (BTP2) (Calbiochem, La Jolla, CA, USA); Fetal calf serum (Biological Industries, Kibbutz Beit Haemek, Israel); fura-2 acetoxymethyl ester (fura-2 AM) (Dojindo Laboratories, Kumamoto, Japan); 2.5% trypsin (Gibco-BRL, Gaithersburg, MD, USA); Dulbecco's modified Eagle's medium (DMEM) (Nissui, Tokyo, Japan); 2-aminoethyl diphenylborinate (2-APB), GR94800, H89, Hanks' balanced salt solution (Hanks' buffer), penicillin/streptomycin, poly-L-lysine, SB222200, thapsigargin, U73122 and xestospongin C (Sigma Chemical, St. Louis, MO, USA); SP (Peptide Institute, Osaka, Japan); CP96345 (Pfizer Central Research, Groton, CT, USA); DNase (Roche, Basel, Switzerland). Ethyl-1-(4-(2,3,3-trichloroacrylamide)phenyl)-5-(trifluoromethyl)-1H-pyrazole-4-carboxylate (Pyr3) was kindly provided by Prof. Y. Mori of Kyoto University (Japan). All other reagents were of the highest purity available from commercial sources.

2.2. Cell culture

Spinal astrocytes were prepared from spinal cords of neonatal Wistar rats according to a previously reported method (Morioka et al., 2009). In brief, the isolated spinal cords were minced, and then incubated with trypsin and DNase. Dissociated cells were suspended in DMEM supplemented with 10% fetal calf serum and penicillin/streptomycin (100 U/ml and 100 μg/ml, respectively). Thereafter, cell suspensions were plated in 75 cm^2 tissue culture flasks (7.5 to 10×10^6 cells/flask) precoated with poly-L-lysine (10 μg/ml). The cells were maintained in a 10% CO_2 incubator at 37 °C. After 10 days, microglial cells were removed by vigorously shaking the growth flasks. Thereafter, the cells were harvested and replated to 35 mm diameter dishes at a density of 3×10^5 cells/dish, or glass coverslips with a silicon rubber wall (FlexiPERM; Heraeus Biotechnology, Hanau, Germany) at a density of 0.2×10^5 cells/slide. At 3 days post-seeding, the medium was replaced with serum-free DMEM. The cells were used for experiments overnight after the medium change. Prepared astrocytes showed a purity >95% as determined by glial fibrillary acidic protein (GFAP) immunoreactivity. All animal procedures were performed in accordance with the Guide for Animal Experimentation, Hiroshima University and the Committee of Research Facilities for Laboratory Animal Sciences, Graduate School of Biomedical Sciences, Hiroshima University, Japan.

2.3. Measurement of $[Ca^{2+}]_i$ in spinal astrocytes

The measurement of $[Ca^{2+}]_i$ was performed using a previously described method (Miyano et al., 2009). All experiments were performed in Ca^{2+} (1.3 mM)-containing or Ca^{2+}-free Hanks' buffer. Spinal astrocytes were loaded with 5 μM of fura-2 AM in Ca^{2+}-containing Hanks' buffer for 50 min at 37 °C. After washing, the cells treated with either SP or GR73632 in Ca^{2+}-containing or Ca^{2+}-free Hanks' buffer, respectively. The fluorescence intensity was measured with the excitation wavelengths of 340 and 380 nm and the emission wavelength of 510 nm. The video image output was digitized by an Argus Hisca color image processor (Hamamatsu Photonics, Shizuoka, Japan).

2.4. RT-PCR analysis

According to a previously reported method (Morioka et al., 2009), total RNA in astrocytes was prepared and used to synthesize cDNA with MuLV reverse transcriptase (Applied Biosystems, Foster City, CA) and a random hexamer primer (Takara Bio Inc., Shiga, Japan). PCR reactions were performed with the specific primers indicated in Table 1 and AmpliTaq Gold™ (Applied Biosystems) at 95 °C for 10 min followed by 35–40 cycles (Table 1) of denaturation at 95 °C for 30 s, annealing at 57 °C for 30 s, and elongation at 72 °C for 2 min, with a final extension at 72 °C for 5 min. The resulting PCR products were analyzed on a 1.5% agarose gel and had the size expected from the known cDNA sequence.

2.5. Immunofluorescence staining

Cells were washed with PBS(−), fixed with 4% paraformaldehyde, and permeabilized with 0.1% triton-X at room temperature. After blocking with 3% BSA, cells were incubated with a polyclonal antibody against the NK-1 receptor (1:100; Sigma), TRPC3 (1:100; AnaSpec Inc., San Jose, CA), or a monoclonal antibody against GFAP (1:200; Sigma) for 1 h at room temperature. Next, the cells were further incubated with Alexa 546-conjugated anti-rabbit IgG antibody, or Alexa 488-conjugated anti-mouse IgG antibody (1:500, Molecular Probes, Invitrogen, Carlsbad, CA) for 1 hour at room temperature. Immunolabeled cells were visualized under a Zeiss LSM510 META confocal microscope (Carl Zeiss, Jene, Germany).

2.6. Statistical analysis

The data are presented as the means ± S.E.M. of at least three independent experiments. The statistical analysis of all data except for Fig. 3F, was performed by a one-way analysis of variance (ANOVA) followed by Bonferroni's test. In Fig. 3F, *t*-test was used to analyze the differences between the two groups. A probability value (p) of less than 0.05 was considered to be statistically significant.

Table 1
The primer sequences and sizes of PCR products of rat TRPC channels.

Subtypes of TRPC	Forward primers (5′→3′)	Reverse primers (3′→5′)	Size (bp)
C1	TCTGGCCAGTCCAGCTCTAA	CCCTTCATACCACAGCCTCT	682
C2	CCCTGCAACCATGCTCATGT	CTTGAGCTGGACAACGGTCT	609
C3	CTTGATCCAGGCTGGGGAAA	CTTTGGCCCCAAGGTAGTAG	708
C4	CTCGCTCATTGCGCTGTCAA	GTCGATGTGCTGAGAGGCTA	547
C5	GCCAAGCTGAAGGTGGCAAT	AGATCTGCAGAGGCCCTAAG	664
C6	GACTCCTTCAGCCACTCTAG	ACGAGCAGCCCCAGGAAAAT	561
C7	TCCCTTTAACCTGGTGCCGA	TCACCCTCAGGTGGTCTTTG	449

3. Results

3.1. Increase in $[Ca^{2+}]_i$ by spinal astrocytes through NK-1 receptor activation

In the presence of extracellular Ca^{2+}, SP evoked an increase in the $[Ca^{2+}]_i$ in a dose-dependent manner at a concentration range of 1–100 nM as shown in Fig. 1A–C. The Ca^{2+} response rapidly peaked after treatment with SP, and then gradually returned toward the basal level within several minutes. The extent of the SP-induced increase in $[Ca^{2+}]_i$ was calculated using the differences between the fura-2 fluorescence ratio (340/380) of the resting level observed before SP treatment and the peak level obtained after SP treatment (Fig. 1G). Next, we investigated which subtypes of NK receptors were involved in the increase of $[Ca^{2+}]_i$ in cells treated with 100 nM of SP. The SP-induced increase in $[Ca^{2+}]_i$ was completely suppressed by pretreatment with CP-96346 (10 μM), a selective antagonist of the NK-1 receptor (Fig. 1D and H). In contrast, neither GR94800 (10 μM), a selective NK-2 antagonist, nor SB222200 (10 μM), a selective NK3 antagonist, affected the SP-

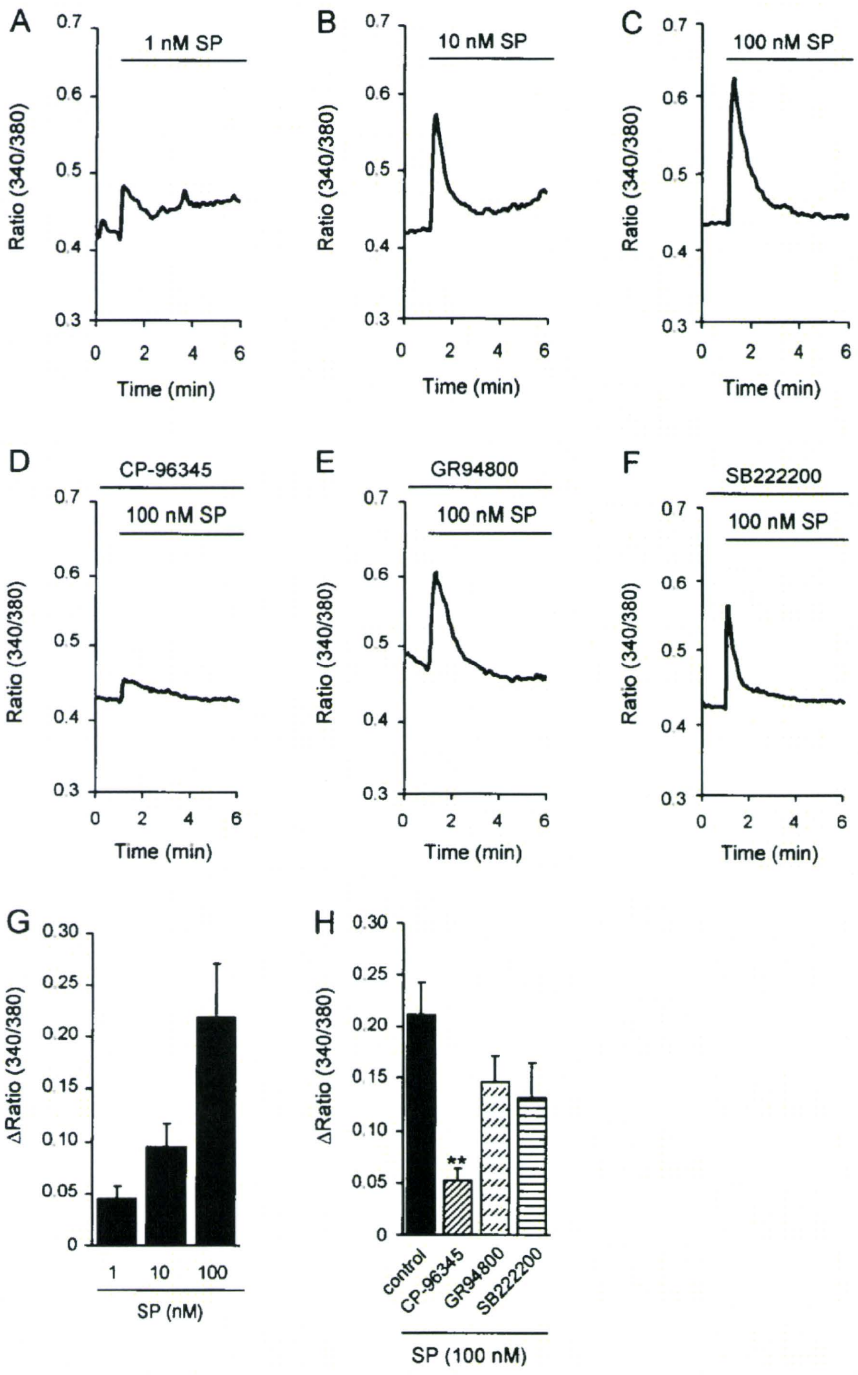

Fig. 1. Mobilization of $[Ca^{2+}]_i$ in spinal astrocytes stimulated with SP. The trace in each graph (A–F) shows the representative mean $[Ca^{2+}]_i$ in randomly selected cells. The fura 2-loaded cells were treated with 1–100 nM of SP in Hanks' buffer, respectively (A–C). After the cells were pretreated with 10 μM of CP96345 (D), GR94800 (E) or SB222200 (F) for 20 min, then cells were stimulated with 100 nM of SP. The extent of the increase in $[Ca^{2+}]_i$ induced by SP was quantified by determining the differences between the ratio (340/380) of the basal and the peak level obtained after SP treatment (G and H). The data are expressed as the means ± S.E.M. (*bars*) of separate experiments. $^{**}p < 0.01$ in comparison with the value for the cells treated with SP alone.